Phase diagram of static- and dynamic-domain formation in weakly coupled GaAs/AlAs superlattices

Naoki Ohtani and Norifumi Egami

ATR Adaptive Communications Research Laboratories, Hikaridai, Seika-cho, Soraku-gun, Kyoto 619-0288, Japan

Holger T. Grahn and Klaus H. Ploog

Paul-Drude-Institut für Festkörperelektronik, Hausvogteiplatz 5-7, D-10117 Berlin, Germany
(Received 1 June 1999; revised manuscript received 13 August 1999)

We report on the phase diagram of static- and dynamic-domain formation in weakly coupled GaAs/AlAs superlattices (SL's). We have performed a detailed investigation of self-oscillations of the photocurrent using the control parameters of applied bias and carrier density inside the SL's. The resulting phase diagram clearly demonstrates that the boundary between oscillating- and static-domain formation, defined as a critical carrier density, varies with bias voltage.

Static electric field domain formation in weakly coupled semiconductor superlattices (SL's) is known to lead to a series of current branches in the time-averaged current-voltage characteristics when the current density is very large.[1,2] However, recent theoretical studies have clarified that the formation of static electric field domains becomes unstable when the carrier density is lower than a critical value. This instability results in spontaneous current oscillations,[3] which have been experimentally observed both in doped[4,5] and undoped, photoexcited[6,7] SL's. The oscillations originate from a recycling motion of the domain boundary, when the carrier density is not sufficiently large to form static domains. In addition, for very low carrier densities, the formation of unstable domains becomes impossible, i.e., no current oscillations are observed.[8] Very recently, numerical calculations have predicted that the boundary between the oscillatory and static regimes does not occur at the same carrier density for different bias voltages.[9] The results of the calculation are also compiled in a phase diagram exhibiting a jagged boundary between oscillatory and static regimes in the parameter space of carrier density versus applied voltage due to the presence of Hopf tongue crossings. Moreover, these calculations have clarified the carrier density dependence of the oscillation frequencies and amplitudes. At the same time, the results of another numerical model have been reported showing that the oscillatory behavior is strongly affected by structural imperfections inside the SL, such as interface roughness and doping fluctuations.[10,11] Accordingly, the phase diagram, i.e., oscillatory regime in the parameter space of carrier density and applied voltage, may be affected.

In this paper, we present experimentally obtained phase diagrams of domain formation in SL's. In undoped, photoexcited systems, the carrier density dependence of the current oscillations can be measured in a single sample by simply varying the excitation intensity. The measured phase diagrams clearly demonstrate that the boundary between the oscillating and static regime depends on carrier density and applied voltage. At the same time, the dependence of the oscillation amplitudes on these two parameters becomes visible.

The investigated sample consists of a nominally undoped, 40-period SL with 9.0 nm GaAs wells and 4.0 nm AlAs barriers embedded in a p-i-n diode processed into a 50 μm square mesa. A cw He-Ne laser beam is focused by a $10\times$ objective lens onto the p-cap layer (beam diameter about 20 μm) to photoexcite carriers in the intrinsic region. The two-dimensional carrier density in the SL region is estimated to be of the order of 10^{11} cm^{-2} per 1 mW laser excitation. The sample is mounted in a closed-cycle cryostat. The frequency spectra of the photocurrent (PC) oscillations are detected with an HP 8566B spectrum analyzer. All measurements have been performed in reverse bias, where no carriers are injected from the contacts of the p-i-n diode.

For a laser intensity of 2.5 mW, oscillations are detected in a wide range of bias voltages between 5.46 and 6.64 V, as shown in Fig. 1(a). The darker areas correspond to larger amplitudes of the current oscillations. The frequency spectra also show the presence of higher harmonics. However, in this paper, we will focus on the fundamental frequency of the current oscillations. In order to derive a phase diagram of dynamic- and static-domain formation, we extract the maximum amplitude of the fundamental frequency at each laser intensity as a function of reverse bias voltage. Figure 1(b) depicts this maximum value of the amplitude as derived from Fig. 1(a). Our investigation focuses on the voltage regime between 5.3 and 6.7 V, because this sample reveals self-sustained PC oscillations only in this voltage region corresponding to the second plateau region of the time-averaged PC-V characteristic. Details of the oscillating mechanism for this sample can be found in Ref. 6.

By performing the same procedure as for Fig. 1(b) for each laser intensity, we can derive the phase diagrams shown in Figs. 2(a) and 2(b) at 20 and 60 K, respectively, where the oscillation amplitude is plotted as a function of reverse bias voltage, i.e., electric field, and laser intensity, i.e., carrier density. The laser intensity has been changed in steps of 0.25 mW. The darker the points in the phase diagram, the larger the oscillation amplitude. At 20 K, the photocurrent oscillations are observed for laser intensities above 0.25 mW. At 0.50 mW, two oscillatory windows are detected near 5.65 and 6.2 V. With increasing carrier density, the two oscilla-
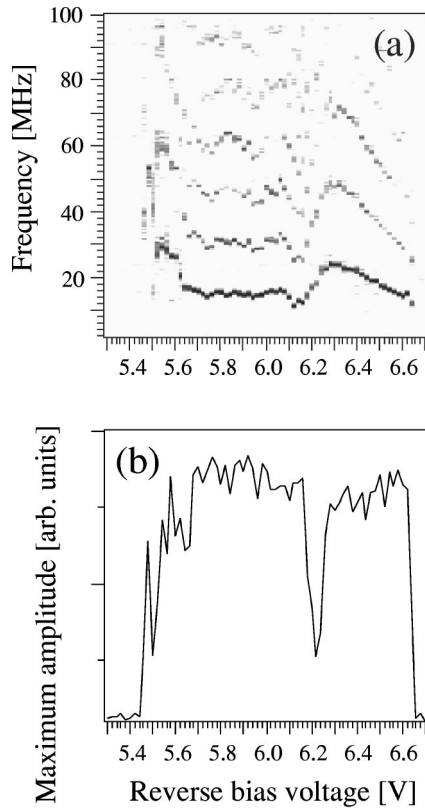
FIG. 1. (a) Frequency spectra of self-sustained photocurrent os-
cillations vs bias voltage for a laser intensity of 2.5 mW at 20 K.
The darker areas correspond to larger amplitudes. (b) Maximum
amplitude of the frequency spectra vs bias voltage under the same
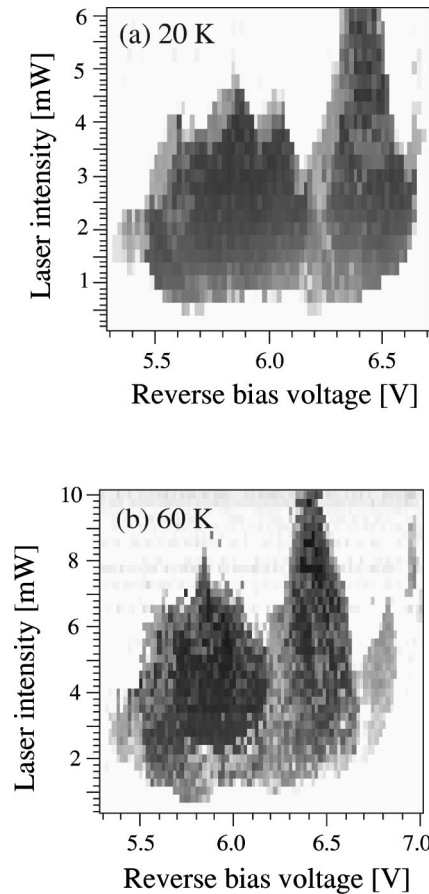conditions as in (a).

FIG. 2. Phase diagram of static and dynamic domain formation
for two different temperatures (a) 20 K and (b) 60 K. The laser
intensity is varied in 0.25 mW steps. The darker areas correspond to
the maximum amplitude of the oscillations at each bias voltage for
each laser intensity.

tory windows become wider and eventually merge, resulting
in oscillations over a wide voltage region. This result indi-
cates that at each bias voltage, the transition between the
static system and the unstable one can occur at different car-
rier densities. Furthermore, the corresponding carrier densi-
ties, where the oscillations begin for each bias voltage, are
bifurcation points as predicted by the calculations.[9]

With a further increase of the carrier density, the width of
the oscillatory window decreases. For a laser intensity of
3.25 mW, a static region without any oscillations appears at
6.15 V, which divides the oscillatory regime into two re-
gions. A further increase in the carrier density results in ad-
ditional islands of stability. Their respective widths increase
with increasing laser power. In order to investigate the de-
tails of the applied voltage dependence of the transition be-
tween static and unstable electric field domain formation for
higher laser intensities, for example, frequency spectra and
the corresponding maximum value of the amplitude of pho-
tocurrent oscillations vs applied voltage for a laser intensity
of 4.25 mW are plotted in Fig. 3. The maximum value of the
amplitude shown in Fig. 3(b), which can be derived from the
phase diagram in Fig. 2(a), clearly exhibits several oscilla-
tory windows and static regions. The boundary between
them can be regarded as a set of Hopf bifurcation points,
because our observation agrees well with the results of the
calculations.[9] Thus, the observed transition between static
and unstable domain formation as a function of applied volt-
age for larger carrier densities is probably a result of the

appearance and disappearance of Hopf tongue crossings as
predicted in the calculations. For laser intensities above 5
mW, only one oscillatory window remains at around 6.4 V.
Above 10 mW, the photocurrent oscillations completely dis-
appear over the whole voltage region. The corresponding
carrier densities, for which each Hopf tongue disappears and
the current oscillations also vanish, are most likely deter-
mined by stationary saddle nodes.[8,9] Note that for all laser
intensities, the oscillation amplitude at 6.2 V is drastically
reduced. At the same time, the frequency also changes, as
evident from Fig. 1(a). This change in the phase diagram
may be caused by growth-related imperfections such as
slight fluctuations in layer thicknesses.[10] We conclude that
the phase boundary between dynamic- and static-domain for-
mation as defined by a critical carrier density, for which the
current oscillations disappear, depends on the applied elec-
tric field and can exhibit a rather jagged shape.

As previous investigations have shown, a higher sample
temperature can result in a wider voltage range, over which
oscillations are present. We therefore performed the same
experiment for a temperature of 60 K, where oscillations are
present between 5.3 and 6.95 V. The resulting phase diagram
is shown in Fig. 2(b). Qualitatively, the phase diagram of
static- and dynamic-domain formation appears to be very
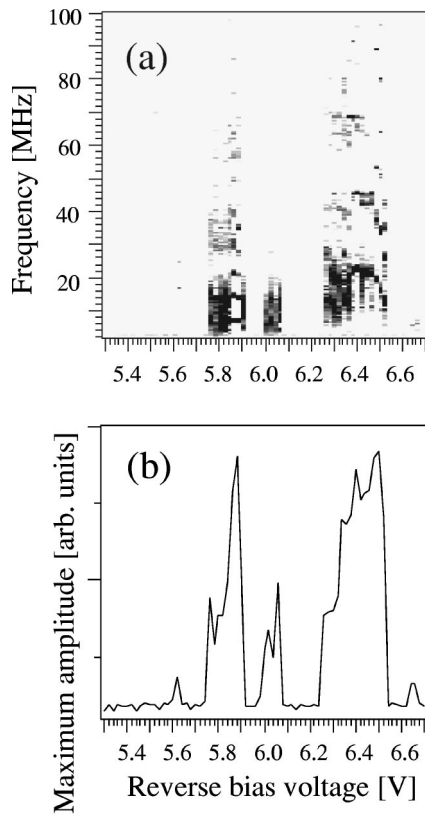similar to the one at 20 K. However, a detailed comparison

FIG. 3. (a) Frequency spectra of self-sustained photocurrent oscillations vs bias voltage for a laser intensity of 4.25 mW at 20 K. The darker areas correspond to larger amplitudes. (b) Maximum amplitude of the frequency spectra vs bias voltage under the same conditions as in (a).

FIG. 4. Carrier density dependence of the maximum amplitude for reverse bias voltages of (a) 5.88 V and (b) 5.76 V at 20 K derived from Fig. 2(a).

also reveals some pronounced differences. The oscillations appear for higher laser powers, (between 0.75 and 15 mW), i.e., the carrier density has to be larger at higher temperatures. At higher temperatures, a thermal activation effect is probably responsible for the destruction of static domain formation,[6] thus resulting in photocurrent oscillations, which are observable over a wider carrier density and wider bias voltage range at higher temperatures. This may be a result of an extension of the Hopf tongues constructing the oscillatory regime by thermal activation, resulting in a wider oscillatory regime. Furthermore, for laser intensities between about 7 and 9 mW, an additional oscillatory window appears at around 6.95 V, where no oscillatory window is detected at 20 K. This behavior probably demonstrates that a new Hopf tongue is generated by thermal activation. Furthermore, the jagged shape of the upper phase boundary is less pronounced [cf. voltage regions between 5.5 and 6 V in Figs. 2(a) and 2(b)]. This probably indicates that the phase boundary for large carrier densities (i.e., saddle-node bifurcation) is very sensitive to temperature. Thus, the fine structure of the upper phase boundary can be easily destroyed for higher temperatures. However, the smaller amplitude regime around 6.2 V is also detected, indicating that the structural imperfections inside the SL can influence the oscillatory behavior even at higher temperatures.

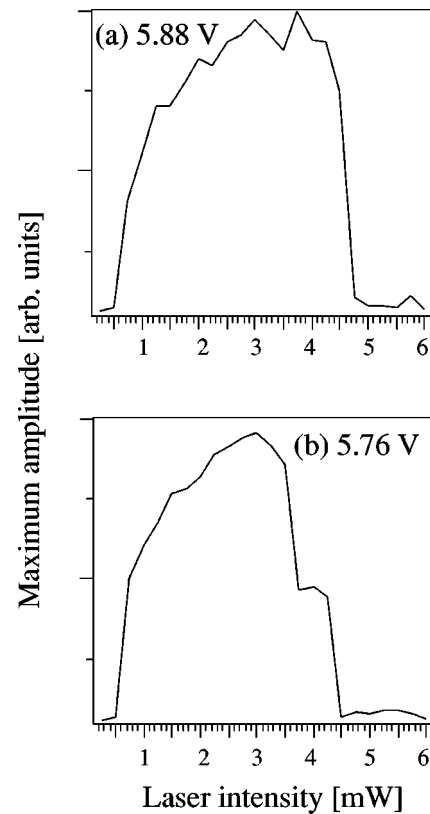From the phase diagrams, we can directly obtain the carrier density dependence of the maximum amplitude of the fundamental oscillations. In Fig. 4(a), the maximum amplitude is shown as a function of the laser intensity (i.e., carrier density) for a reverse bias voltage of 5.88 V derived from Fig. 2(a). The oscillations begin at 0.75 mW. With increasing laser intensity, the maximum amplitude gradually increases reaching a maximum between 2.5 and 4 mW. A further increase of the laser intensity results in a steep decrease of the amplitude. At 4.75 mW, the oscillations have completely disappeared. Since the oscillation frequency decreases with increasing carrier density,[6,7] while the amplitude remains almost constant just before the disappearance of the oscillation, the observed bifurcation is a homoclinic connection, as predicted by the calculations.[9] However, even a small change in the reverse bias voltage can sometimes result in a drastic change of the carrier density dependence of the maximum amplitude due to the presence of undriven chaotic oscillations.[12,13] Figure 4(b) shows the laser intensity dependence of the maximum amplitude for a smaller bias voltage of 5.76 V, also derived from Fig. 2(a). When at large carrier densities the oscillation amplitude decreases towards zero, a steplike behavior is clearly detected for laser intensities near 4 mW. In this plateau, the SL exhibits undriven chaotic oscillations, whose corresponding frequency spectra are shown in Fig. 3(a), where broadened spectra are detected. In the phase diagram in Fig. 2(a), undriven chaos usually appears on the lower voltage side in each oscillatory window. We believe that the appearance of these chaotic windows is connected with the presence of negative differential conductance (NDC) regimes in the time-averaged photocurrent-voltage characteristics.[6,12,13]

In summary, the phase diagram of dynamic- and static-

domain formation in a weakly coupled SL is derived by performing a detailed investigation of the frequency spectra of the photocurrent oscillations as a function of laser intensity (i.e., carrier density) and reverse bias voltage (i.e., electric field). The boundary between dynamic- and static-domain formation is clearly not voltage independent, but shows rather a jagged shape. For some bias voltages, the oscillation regime extends much further than for most other ones.

[1] L. Esaki and L. L. Chang, Phys. Rev. Lett. **8**, 496 (1974).

[2] H. T. Grahn, R. J. Haug, W. Müller, and K. Ploog, Phys. Rev. Lett. **67**, 1618 (1991).

[3] L. L. Bonilla, in *Nonlinear Dynamics and Pattern Formation in Semiconductors and Devices*, edited by F.-J. Niedernostheide (Springer-Verlag, Berlin, 1995), Chap. 1.

[4] H. T. Grahn, J. Kastrup, K. Ploog, L. Bonilla, J. Galán, M. Kindelan, and M. Moscoso, Jpn. J. Appl. Phys., Part 1 **34**, 4526 (1995).

[5] J. Kastrup, R. Hey, K. H. Ploog, H. T. Grahn, L. L. Bonilla, M. Kindelan, M. Moscoso, A. Wacker, and J. Galán, Phys. Rev. B **55**, 2476 (1997).

[6] N. Ohtani, N. Egami, H. T. Grahn, K. H. Ploog, and L. L. Bonilla, Phys. Rev. B **58**, R7528 (1998).

[7] K. J. Luo, S. W. Teitsworth, H. Kostial, H. T. Grahn, and N. Ohtani, Appl. Phys. Lett. **74**, 3845 (1999).

[8] A. Wacker, M. Moscoso, M. Kindelan, and L. L. Bonilla, Phys. Rev. B **55**, 2466 (1997).

[9] M. Moscoso, J. Galán, and L. L. Bonilla, in Proceedings of the 24th International Conference on the Physics of Semiconductors, edited by D. Gershoni (World Scientific, Singapore, in press). Paper no. V-C-14, PDF file no. 0524.pdf on the CD ROM.

[10] E. Schöll, G. Schwarz, and A. Wacker, Physica B **249-251**, 961 (1998).

[11] M. Patra, G. Schwarz, and E. Schöll, Phys. Rev. B **57**, 1824 (1998).

[12] Y. Zhang, R. Klann, H. T. Grahn, and K. H. Ploog, Superlattices Microstruct. **21**, 565 (1997).

[13] N. Ohtani, N. Egami, H. T. Grahn, and K. H. Ploog, Physica B **249-251**, 878 (1998).